Carbohydrate Polymers 113 (2014) 46–52

Contents lists available at ScienceDirect

Carbohydrate Polymers

journal homepage: www.elsevier.com/locate/carbpol

Natural polymer biocomposites produced from processing raw wood flour by severe shear deformation

Xiaoqing Zhang[a,*], Xiaolin Wu[b], Hengky Haryono[b], Kenong Xia[b,**]

[a] CSIRO Materials Science and Engineering, Private Bag 33, Clayton South MDC, VIC 3169, Australia
[b] Department of Mechanical Engineering, The University of Melbourne, VIC 3010, Australia

ARTICLE INFO

Article history:
Received 27 May 2013
Received in revised form
20 September 2013
Accepted 19 June 2014
Available online 9 July 2014

Keywords:
Biocomposites
Natural polymer
Powder processing
Mechanical properties
Phase structures

ABSTRACT

Wood flour (WF) based natural polymer biocomposites were produced using the equal channel angular pressing (ECAP) technique. The wood particle structures were disrupted and the cellulose crystallinity was decreased while bulk materials were formed with continuous phase structures by the severe shear-deformation during ECAP. The mechanical properties of the processed WF materials were enhanced when the processing temperature was increased due to enhanced intermolecular interactions and thermal crosslinking reactions among WF components. The processing capability was improved by using wheat gluten (WG) as additives, leading to significantly reduced processing temperature. Effective chain penetration and strong intermolecular interactions in conjunction with chemical crosslinking occurred between WG and the amorphous components in WF. However, the thermal decomposition of the WG component also occurred at increased temperatures, resulting in a decrease in the mechanical strength of the WF/WG composites. The result has demonstrated that ECAP is a promising methodology to produce renewable and degradable biocomposites from wood waste.

1. Introduction

Utilizing agricultural waste streams as feedstocks to develop biodegradable and renewable materials will provide great benefit to economics and environment without competing with food and energy consumption of the agriculture products. Continuous attention has been focused on cellulose-based feedstocks as cellulose is the most abundant material in nature with excellent properties in many aspects (Klemm, Heublein, Fink, & Bohn, 2005; Ragauskas et al., 2006). However, cellulose is difficult to be thermally processed without significant chemical modification due to its complicated structure and high crystallinity. It has been mainly used as reinforced additives in polymer composite manufacturing (Bogoeva-Gaceva et al., 2007; John & Thomas, 2008; Lu, Zhang, Rong, Shi, & Yang, 2003; Wang & Zhang, 2009). Recently we have worked on consolidating cellulose particles into bulk plastic materials through equal channel angular pressing (ECAP) under severe shear deformation conditions and received some success (Zhang, Wu, Gao, & Xia, 2012). An efficient deformation of the crystalline structure of cellulose occurred during the process, resulting in the formation of bulk plastic material with effective chain penetration and strong intermolecular interactions throughout the whole material. The processing capability was enhanced when using amorphous natural polymers such as wheat gluten (WG) as an additive, leading to significantly improved mechanical properties (Zhang, Wu, & Xia, 2013). These results demonstrated a promising methodology to produce polymer materials from cellulose-based waste. However, the rigid cellulose with high crystallinity lacks sufficient mobility to cope with the severe shear deformation, and micro-cracking occurred especially at lower processing temperatures, resulting in low mechanical strength when no WG additives were used.

In this study, raw wood flour (WF) was taken as a model cellulose-based waste and processed by ECAP under various conditions. As the crystalline cellulose content in WF is much lower than that in pure cellulose, the material processability is expected to improve. In addition, it would be interesting to investigate the behavior of the important WF components, hemi-celluloses and lignin, during ECAP. The effect of WG additives were also examined since the amorphous material played a role in forming continuous morphologies to further enhance the processability and mechanical properties of cellulose (Zhang et al., 2013). WG itself could also be thermally processed into thermoplastics with excellent properties (Belton, 1999; Zhang, Do, Hoobin, & Burgar, 2006; Zhang, Hoobin,

* Corresponding author. Tel.: +61 3 95452653; fax: +61 3 95441128.
** Corresponding author. Tel.: +61 3 83446664; fax: +61 3 83444290.
E-mail addresses: Xiaoqing.Zhang@csiro.au (X. Zhang), K.Xia@unimelb.edu.au (K. Xia).

http://dx.doi.org/10.1016/j.carbpol.2014.06.076
0144-8617/

Burgar, & Do, 2006). Since both WF and WG are biodegradable, the WF/WG biocomposites would retain the biodegradable and renewable characteristics. The processing methodologies, material morphologies, mechanical properties and glass transition behaviors of the WF and WF/WG composites were examined. Molecular motions, phase structures and intermolecular interactions among WF and those between WF and WG components were also studied and correlated to the material properties.

2. Experimental

2.1. Materials

Maple wood flour (WF) was obtained from American Wood Fibers with a particle size distribution of 850 μm (0–15%), 525 μm (45–90%), 250 μm (5–55%). The WF contains 37–47% of cellulose, 20–30% of hemi-cellulose and 21–34% of lignin on a dry base with 8% of moisture. The raw vital wheat gluten (WG) powder was supplied by Manildra Group Australia as food grade products from commercial processing. The WG contained 80% of proteins, 15% of residual starch, 4% lipid, and 1% of fiber plus other impurities on a dry base. The moisture content in the WG was 9–10%. These samples were processed without any pre-treatment.

2.2. ECAP

The ECAP set-up is the same as described previously (Zhang, Gao, Wu, & Xia, 2008) using the same die with a 90° degree angle between the channels of 9 mm × 9 mm in cross section. The WF or WF/WG mixtures at different proportions were ball-milled for 2 h (a 10 min break in the middle of milling to avoid excessive heating) at a speed of 300 rpm before ECAP. The ratio of the powder sample to steel balls was 1:20 (in weight) and both large and small (7 and 4 mm in diameter, respectively) steel balls (1:1 in weight) were used. The powder samples were pressed at a speed of 25 mm/min with a constant back pressure of 100 MPa. L-shaped bulk cellulose samples with a length of ~50 mm passing the shear plane were produced after ECAP. The samples were then conditioned at room temperature under a relative humidity (RH) of 50 ± 2% (achieved by saturated $Mg(NO_3)_2$ salt solution) for 2 weeks before any testing. The moisture contents of these samples after conditioning were between 7.6 and 8.3 wt% (error bar of 4–5%), measured as weight loss after heating at 105 °C for 5–6 h to reach a constant weight.

2.3. Material characterization

Fracture surfaces of the WF or WF/WG composite samples were produced by bending at a location passing the shear plane in ECAP after they had been chilled in liquid nitrogen, and examined by scanning electron microscopy (SEM) at room temperature using Philips XL30 FEG. The electron beam with an accelerating voltage of 5 kV was used to produce high definition images.

For 3-point bending testing conducted at room temperature, each sample bar was placed on two parallel rollers with a span of 32 mm. The load and displacement were recorded and converted into stress versus strain curves to obtain the flexural strength and elastic modulus. A PerkinElmer PYRIS™ Diamond dynamic mechanical analyzer (DMA) in the single cantilever bending mode was used at a frequency of 1 Hz. The temperature range was set from −100 to 250 °C with a heating rate of 2 °C/min.

High-resolution solid-state NMR experiments were conducted at room temperature either using a Bruker AV500 spectroscopy (125 MHz for ^{13}C and 500 MHz for ^{1}H) or a Varian NMR300 System (75 MHz for ^{13}C and 300 MHz for ^{1}H). ^{13}C NMR spectra were observed under cross polarization (CP), magic angle spinning (MAS) and high power dipolar decoupling (DD) conditions. The 90° pulse for ^{1}H and ^{13}C channels was 2.9 or 5.5 μs for the experiments using Bruker AV500 or Varian NMR300. The spinning rate of MAS was set at 7.5 kHz and a contact time of 1.0 ms was used for measuring all CP/MAS spectra in both spectrometers. The chemical shift of ^{13}C spectra was determined by taking the carbonyl carbon of solid glycine (176.3 ppm) as an external reference standard. ^{13}C CP/MAS spectra of the crystalline components in WF with longer ^{13}C spin-lattice relaxation times ($^{13}C\,T_1$) were detected on the Bruker AV500 NMR spectrometer. The ^{1}H spin-lattice relaxation time in rotation frame ($^{1}H\,T_{1\rho}$) was measured through the change of ^{13}C magnetization prepared by CP after varied ^{1}H spin-locking times on the Varian NMR300 system. ^{13}C solution NMR spectra were also measured using the Varian NMR300 System under high power decoupling conditions.

Table 1
The results of 3-point bending test for ECAP processed WF and WF/WG materials.[a]

Samples	Flexural strength (MPa)	Elastic modulus (MPa)
WF – 185 °C	4.1	626
WF – 210 °C	20.1	1193
WF – 210 °C (no milling before ECAP)	6.6	746
WG-10% – 125 °C	10.1	1066
WG-20% – 125 °C	21.4	2265
WG-30% – 125 °C	25.4	2449
WG-10% – 150 °C	4.3	777
WG-20% – 150 °C	6.7	806
WG-30% – 150 °C	9.6	1162
WG – 130 °C	28.1	1044

[a] Error bar of 6–12%.

3. Results and discussion

The particle size of WF experienced minimal change after the ball-milling as shown in Fig. 1A and B. For the WF/WG mixture (e.g. the 80/20 sample shown in Fig. 1C and D), the milling caused WG particles to stick to the surface of WF. Processing WF by itself resulted in continuous structures of the bulk samples with no observable cracking at 185–210 °C (Fig. 2A–C). However, minor cracking along the shear direction was observed when processing temperature was lower (e.g. 130–150 °C). When amorphous WG was added to the WF, a continuous morphology was formed in the WF/WG samples at temperatures as low as 125 or 150 °C (Fig. 2D and E). However, broken structures of the plastic phase were observed on the fracture surfaces for samples processed at 150 °C at a high magnification (Fig. 2F). These results are similar to those of the cellulose/WG systems (Zhang et al., 2013).

The results of 3-point bending tests for the WF and WF/WG composites are shown in Table 1 with comparison to those of WG processed at 130 °C (Zhang et al., 2008). The flexural strength/modulus of the milled WF processed at 185 °C was weak, but the values increased significantly with increasing processing temperature to 210 °C. However, un-milled WF processed at 210 °C still displayed low flexural strength/modulus, indicating the ball-milling played a key role in disrupting the WF particle surface structures. Although the WF particle size was not decreased during the milling, the fresh disrupted surface would be beneficial for forming enhanced interactions and chain penetration within WF materials during ECAP. When using WG as an additive, the WF/WG composites processed at 125 °C displayed high flexural strength/modulus especially when the amount of WG was 20–30%. Compared to the results of WG-only sample (Zhang et al., 2008), it seems WG acted as a binder in the WF/WG composites, played a key role in flexural strength. An enhanced modulus was also achieved when an efficient chain penetration occurred between WG and amorphous WF (e.g. the systems with 20–30% of WG), significantly higher than that of WG-only system since the theoretical

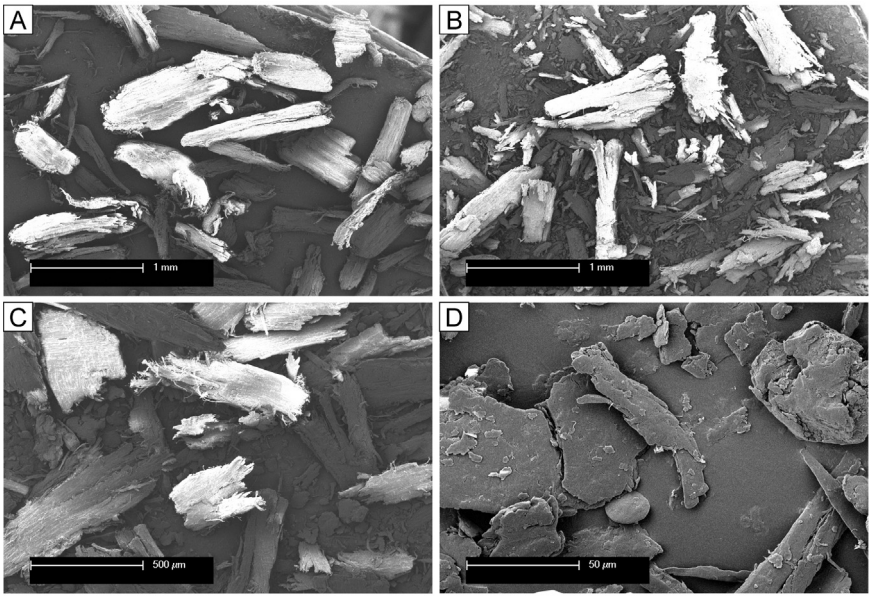

Fig. 1. SEM images of the original raw WF particles (A), milled WF (B) and milled WF/WG = 80/20 mixture on different scales (C and D).

modulus of the cellulose is much higher (Eichhorn & Young, 2001; Tanaka & Iwata, 2006). The strength is comparable or higher than that of the WG composites using a similar amount of jute fibers as reinforcement (Reddy & Yang, 2011). When the WF/WG materials were processed at 150 °C, both flexural strength and modulus were lower than the materials produced at 125 °C, due partially to thermal decomposition of the WG component at higher temperatures as reported previously (Zhang et al., 2008).

The thermal crosslinking between WF and WG may have also contributed to the strength enhancement of the composites. In

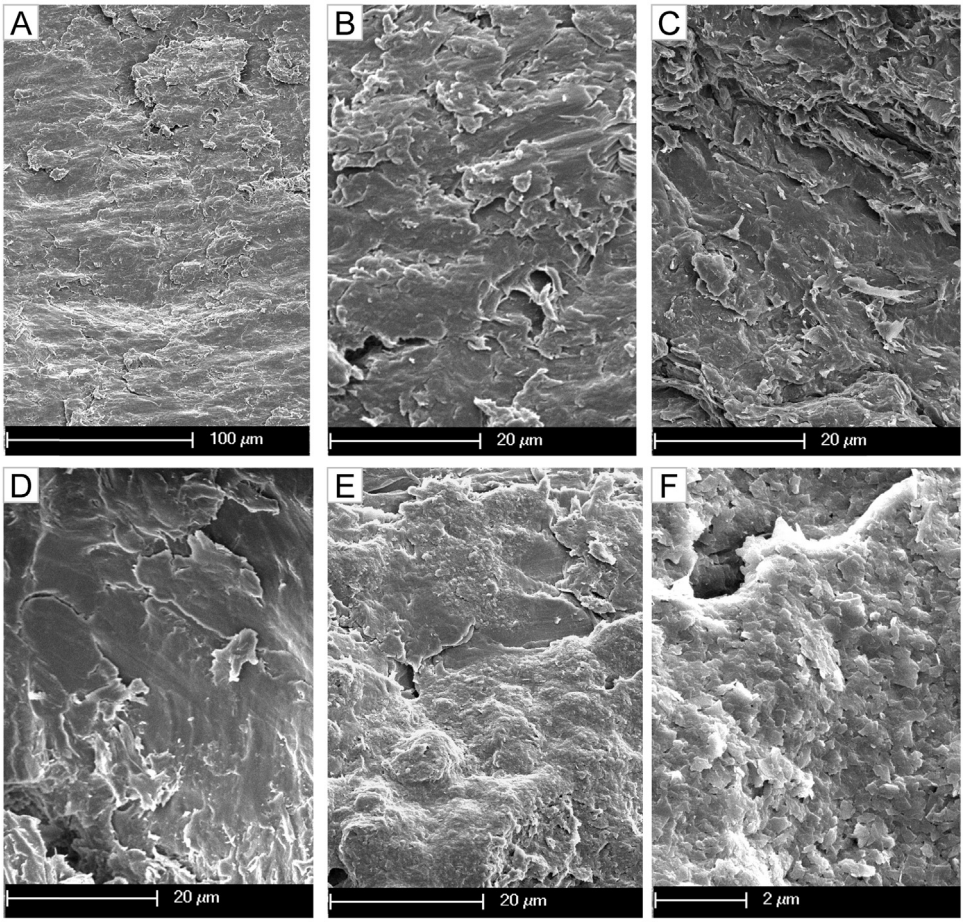

Fig. 2. SEM images of milled WF after ECAP at 185 °C (A), 200 °C (B), 210 °C (C), and milled WF/WG = 80/20 processed at 125 °C (D) and 150 °C on different scales (E and F).

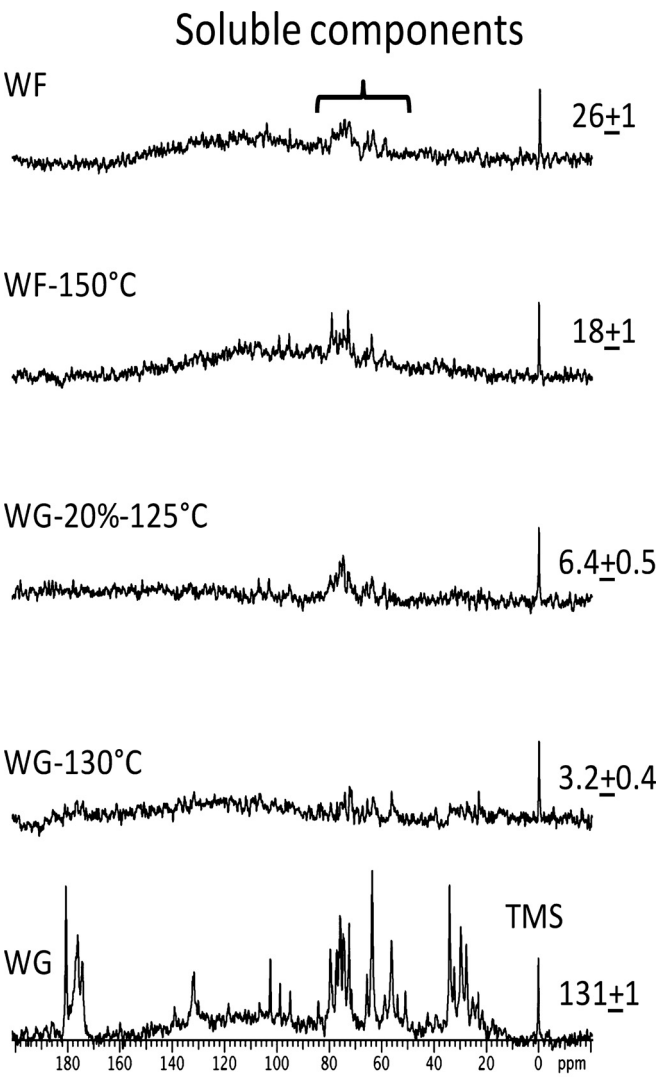

Fig. 3. ^{13}C solution NMR spectra of the soluble components in the original WG (WG), WG after ECAP at 130 °C (WG – 130 °C), original WF (WF), WF after ECAP at 150 °C (WF-150 °C), and WF/WG = 80/20 composite after ECAP at 125 °C (WG-20% – 125 °C). The values next to the TMS peaks are the relative intensities of the soluble components observed in the range of 50–90 ppm.

order to examine the effect, original WF and WG as well as ECAP processed WF, WG and WF/WG composites were soaked in distilled water (6% solid) under sonication for overnight. These water solutions were then examined by ^{13}C solution NMR spectroscopy using tetramethylsilane (TMS) in a constant concentration as internal intensity reference, and the results are shown in Fig. 3. It is noted that WG before ECAP was a partially soluble material with high intensities of soluble proteins and starch over a broad chemical shift range. After ECAP at 130 °C, the intensities of soluble components were decreased significantly especially for the protein components. Soluble starch were still observed but its relative intensity (to TMS) in the range of 50–90 ppm decreased from 131 (before ECAP) to only 3.2 (after ECAP). The result indicates that thermal crosslinking generated a polymer network throughout the whole WG material with only a few soluble components remaining in the system. The solubility of WF in water was low; the relative intensity of the soluble components in the range of 50–90 ppm (mainly soluble hemicelluloses) was 26 (before ECAP). It only decreased moderately to 18 after ECAP at 150 °C, but further decreased to 5–8 after ECAP at >185 °C (spectra not shown), suggesting the enhanced thermal crosslinking effect at higher ECAP temperatures. For the WF/WG composites processed at 125 °C, the relative intensities of the soluble components were around 6–8 (only the ^{13}C NMR spectrum for WF/WG = 80/20 is shown in Fig. 3 as WG – 20–125 °C), suggesting that a high degree of thermal crosslinking occurred throughout the whole WF/WG composites between the WF and WG components during ECAP.

The DMA results of the ECAP processed WF and WF/WG samples are shown in Fig. 4. Similar to normal polymers, the storage modulus E' experienced little change as temperature increased below the glass transition temperature (T_g), and then dropped at a critical temperature at the start of T_g, while a tan δ (loss modulus E''/storage modulus E') peak was observed corresponding to the transition. Note that the E' values of the WF below T_g (ca 20 °C) were significantly increased when the processing temperature was increased (Fig. 4 left). A similar E' increase was achieved by increasing the amount of WG in the WF/WG composites processed at 125 °C (Fig. 4 right). Note that the E' values of all WF/WG samples at 20 °C are lower than that of the WG-only sample processed at 130 °C (Zhang et al., 2008), and this is different from the 3-point bending results, possibly attributed to the different mechanisms of the deformation.

A minor transition was observed on the tanδ curves for WF samples starting at ~50 °C, which could be attributed to the segmental motions of the amorphous phase (hemi-cellulose). The tanδ intensity of such a transition was decreased when processing temperature was increased due to thermal crosslinking among different components in WF. When WG was used, this transition was overlapping with the T_g transition of WG component (starting at ~60 °C) with tanδ intensity increased slightly for the WF/WG samples containing 20–30% of WG. The tanδ peak corresponding to the T_g of WF appeared at 215–220 °C, but it shifted to 185–190 °C when WG was added in the composites. The WG was plasticized with the ~8% moisture content, thus its T_g was decreased (Zhang, Do, et al., 2006; Zhang, Hoobin, et al., 2006). The intensities of the WF tanδ peaks decreased as the processing temperature increased, showing another evidence of the thermal crosslinking effect on restriction of chain motions in WF at the T_g transition. The addition of WG slightly enhanced the chain motions at the T_g of the WF/WG composites as reflected by the increase in tanδ intensities, being consistent with the contribution from the WG component. The DMA results suggest that WG and the amorphous components in WF were intimately mixed through strong intermolecular interactions and thermal crosslinking between the two components. The enhancement of chain mobility at T_g for WF/WG composites could be attributed to the low crystallinity in WF (as compared to microcrystalline cellulose (Zhang et al., 2012) which would be studied by high-resolution solid-state NMR.

The ^{13}C CP/MAS NMR spectra of the original WF powders and those milled then processed at 185 and 210 °C, respectively, are shown in Fig. 5A. The strong resonances at 21, 50–110 ppm are mainly attributed to cellulose and hemicellulose while the weak resonances are due to the C=O (175 ppm) and aromatic (130–140 ppm) structures of lignin. The relatively strong intensity at 155 ppm indicates syringyl units were predominant in the lignin that found in hard wood lignin (Sjostrom, 1993). Fig. 5B displays the ^{13}C NMR spectra of the WF components with a long ^{13}C T_1 relaxation time as detected by the Torchia pulse sequence with a long delay time (τ = 50 s) (Zhang et al., 2012; Zhang et al., 2013). The ^{13}C T_1 is sensitive to molecular motions of different groups in different phases due to the ^{13}C rare unclear system without spin-diffusion interactions. In general, a longer ^{13}C T_1 value is obtained for carbon resonances with no directly bonded hydrogen, or for those in the crystalline phases. Note that the WF spectra (Fig. 5B) remained similar after ECAP, except that the linewidth became a bit broader after processing at higher temperatures, indicating that the cellulose I type character (Horii, Hirai, & Kitamaru, 1987; Newman, 1999; Nishino, Matsuda, & Hirao, 2004; VanderHart & Atalla, 1984)

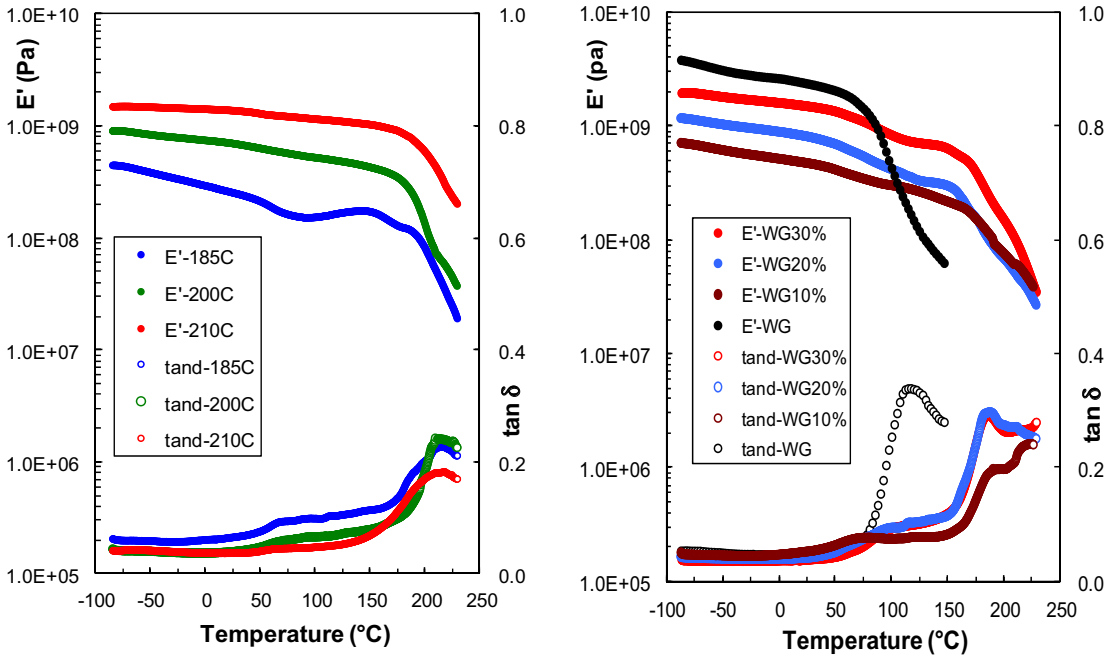

Fig. 4. DMA results of the ECAP processed WF (left) and WF/WG materials processed at 125 °C (right).

remained in the WF components after ECAP while the crystalline size and regularity might have been modified.

The ^{13}C CP/MAS NMR spectra of the WF/WG composites are shown in Fig. 6 and compared with those of original WF and WG powders. For the WG component, the resonance at 175 ppm was due to the C=O in WG, while the resonances at 50–60 and 30–15 ppm were assigned to the C-α, C-β and C-γ resonances of the proteins (Zhang, Hoobin, et al., 2006; Zhang et al., 2008). The minor resonances of residual starch (15 wt% in WG) overlapped with those of cellulose and hemi-cellulose. After ECAP, the linewidth of most WG resonances in the WF/WG samples became broader, suggesting the formation of a broad distribution of chemical environment of the component, evidenced by strong intermolecular interactions with the amorphous cellulose component in conjunction with thermal crosslinking and decompositions.

As described previously (Newman, 1999; Nishino et al., 2004), the separation of the C-4 resonance of cellulose was due to the crystalline (91 ppm) and the amorphous (85 ppm) phases, and their relative intensities could be used to estimate the crystallinity of the cellulose component in the WF materials. For the WF/WG materials, the effect of weak resonance of starch at 83 ppm could be ignored especially when the WG content is low (e.g. WF/WG = 90/10), thus

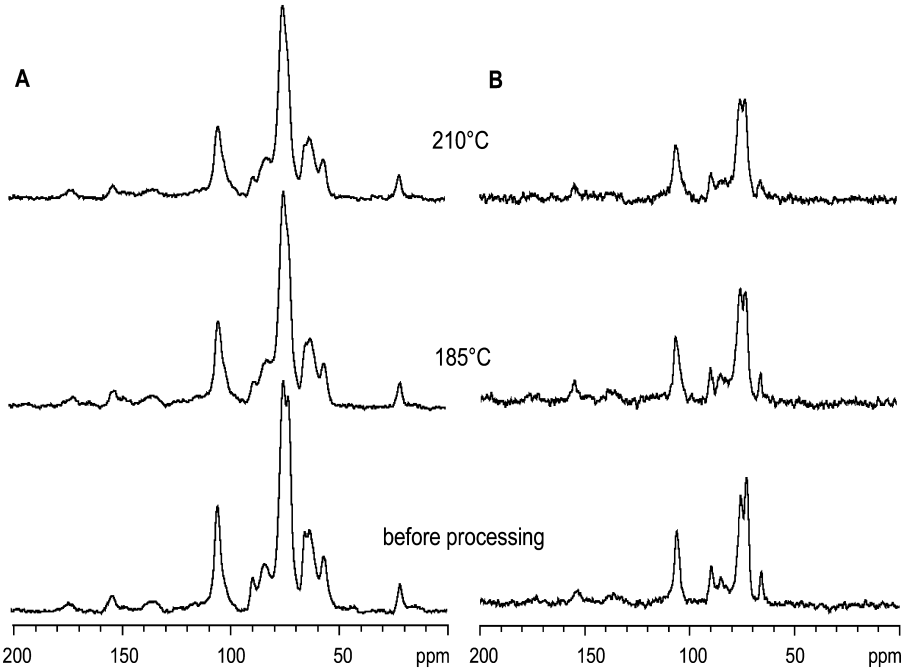

Fig. 5. ^{13}C CP/MAS spectra of milled WF (before ECAP) and those ECAP processed at 185 °C and 210 °C observed by normal CP/MAS pulse sequence (A) or by Torch pulse sequence with delay time $\tau = 50$ s (B).

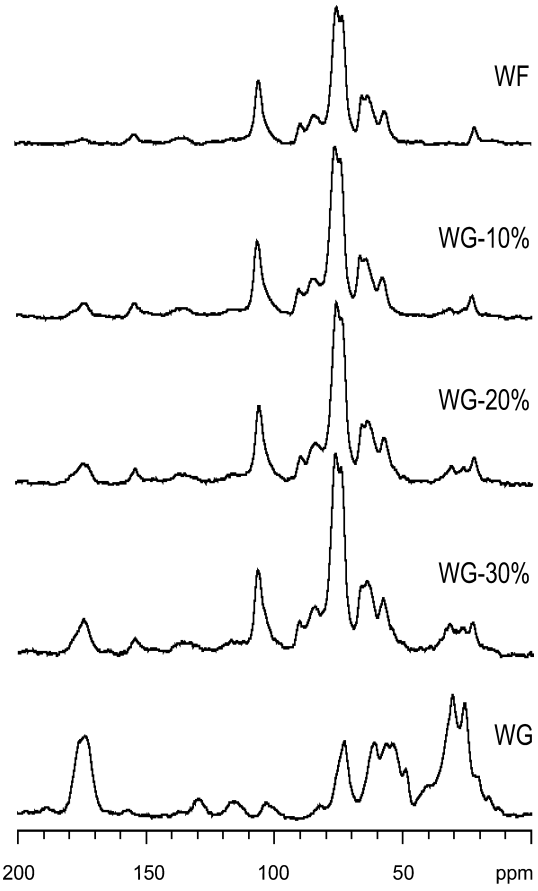

Fig. 6. ^{13}C CP/MAS spectra of milled WF and WG powers before processing and WF/WG materials processed at 125 °C by ECAP.

the crystallinity data obtained would reflect the crystallinity for the WF component only, not for the whole WF/WG materials. In the systems containing a high amount of WG, these residue starch signals might contribute to the intensities of amorphous cellulose, leading to a slightly under-estimated crystallinity. For WF only systems, the crystallinity of WF did reduce from ~21% (after milling) to 14–15% after ECAP at high processing temperatures (200–210 °C), suggesting the crystalline structures was indeed disrupted to some extend by the severe shear deformation. However, for WF/WG systems, the crystallinity in the WF component remained at ~21%, the same as that in the original milled WF, indicating the shear deformation effect on the cellulose crystalline phase was not significant due to the existence of the amorphous WG components, following the same trend as that in the cellulose/WG system (Zhang et al., 2013).

High-resolution solid-state NMR also provides a powerful technique to examine the molecular motions in different components at varied frequencies through measuring relaxation times, and the homo- or heterogeneity of the system on a scale of effective spin-diffusion length during the relaxation time for rigid polymer systems. The ^{1}H spin–lattice relaxation times in rotating frame ($T_{1\rho}$) for WF samples are shown in Table 2. Note that the $T_{1\rho}$ values observed for the cellulose/hemi-cellulose (103–55 ppm) slightly decreased after ECAP at 185 °C but further increasing the processing temperature caused no further change for the values, suggesting the cellulose and hemi-cellulose components were relatively stable when processing at 200–210 °C. However, the data for the lignin component (20, 134–175 ppm) slightly increased after processing at 185 °C, but further increase was significant when processing WF at 210 °C, indicating a considerable change

Table 2
^{1}H $T_{1\rho}$ (ms) of milled and ECAP processed WF materials.[a]

	Samples		
	WF-milled	WF – 185 °C	WF – 210 °C
175 ppm	5.0	5.9	10.5
155 ppm	4.6	6.3	11.1
134 ppm	5.2	6.2	9.8
103 ppm	10.1	8.4	8.5
73 ppm	9.4	8.3	8.4
62 ppm	10.2	8.4	8.3
55 ppm	10.1	8.3	8.5
20 ppm	4.9	8.2	10.2

[a] Error bar of 3–6% for resonances at 55–103 ppm, and 9–14% for the resonances at 20, and 134–175 ppm.

in molecular motions in the lignin component at high temperatures, possibly due to crosslinking reactions most likely at the *ortho* un-substituted positions of the phenolic rings because the *para* positions were substituted in lignin (Sjostrom, 1993). Many components such as proteins, starch and cellulose could participate in the reactions at high temperatures following different chemical pathways (Zhang & Solomon, 1998; Zhang, Hoobin, Burgar, & Do, 2006c; Zhang et al., 2010).

The ^{1}H $T_{1\rho}$ data observed at 155 ppm, 73–103 ppm and 28 ppm can be taken to study the motional changes of the lignin and cellulose/hemi-cellulose in the WF and WG components, respectively, since they do not overlap with the resonances of the other components (Fig. 6). These data are listed in Table 3 and compared with those of the WG-only sample processed at 130 °C. There was no significant change in the ^{1}H $T_{1\rho}$ data for the cellulose/hemi-cellulose components (at 73 and 103 ppm) in the WF/WG composites after processing at 125 or 150 °C, but the data for lignin (at 155 ppm) and WG (at 28 ppm) in the WF/WG systems significantly increased after processing at 150 °C. These results suggested that the lignin and WG components could be modified more significantly at higher temperature by ECAP. An increase in temperature could enhance the chain mobility, resulting in efficient chain penetration and enhanced intermolecular interactions among these components. Thermal crosslinking and decomposition were also enhanced, impacting on mechanical properties of the materials. It seems that the thermal crosslinking was the main effect occurring in lignin or between lignin and other components when processing temperature was increased. When WG was used, the crosslinking (including those between lignin and WG components) would certainly be enhanced at increased temperature, but the low thermal stability of WG could have played a predominant role causing a decrease in mechanical strength of the WF/WG composite at 150 °C.

The ^{1}H $T_{1\rho}$ values also provided structure and phase information on a scale of 2–3 nm, the spin-diffusion length during the ^{1}H $T_{1\rho}$ relaxation time within 10 ms. The significant variation in ^{1}H $T_{1\rho}$ among different components of the WF/WG composites indicates that the materials are heterogeneous systems but with strong intermolecular interactions and crosslinking between the two components.

This study using WF as a model cellulose waste has provided further promising results, indicating that ECAP could be an effective methodology to process wood waste into plastic bulk materials. The amorphous component hemi-cellulose or lignin in the wood would act as useful additives/crosslinkers to improve the processing capability and mechanical properties of the biocomposites. The addition of amorphous natural polymer can further enhance the processability and reduce processing temperature. Pre-milling seems necessary to provide fresh disrupted surfaces for effective chain penetration during ECAP. Future work will be focused on examining the effect of the degree of shear deformation

Table 3
^{1}H $T_{1\rho}$ (ms) of WF, WG and WF/WG composites.[a]

	Samples								
	WF-milled	WF – 185 °C	WG-10% – 125 °C	WG-20% – 125 °C	WG-30% – 125 °C	WG – 130 °C	WG-10% – 150 °C	WG-20% – 150 °C	WG-30% – 150 °C
175 ppm	5.0	5.9	5.4	5.4	5.5	3.6	5.8	6.0	6.4
155 ppm	4.6	6.3	5.0	5.0	5.3	–	6.4	6.8	7.1
134 ppm	5.2	6.2	5.4	5.5	5.5	–	6.5	6.2	7.2
103 ppm	10.1	8.4	11.5	11.0	10.1	3.5	11.1	11.2	11.4
73 ppm	9.4	8.3	11.0	9.7	9.4	3.4	11.2	10.9	11.2
28 ppm	–	–	4.0	4.5	4.6	3.6	5.4	6.0	6.1
20 ppm	4.9	8.2	5.1	5.4	5.3	3.6	6.0	5.8	5.9

[a] Error bar of 3–6% for resonances at 73–103 ppm, and 9–14% for the resonances at 20, 28 and 134–175 ppm.

and developing thermally stable amorphous natural polymer additives, leading to scale-up for industrial applications.

4. Conclusions

The success in processing WF into bulk biocomposites has demonstrated that ECAP is an effective method to process cellulose-based raw wood waste into biodegradable and renewable bulk materials. When increasing the processing temperature, the chain penetration and thermal crosslinking between WF components were enhanced, generating increased mechanical strength. The amorphous component, hemi-cellulose or lignin, in WF acted as useful additives or crosslinkers to improve the processability or mechanical properties of the biocomposites. The addition of amorphous natural polymer such as WG would further enhance the processing capability and reduce the processing temperature to as low as 125 °C. Strong intermolecular interactions and crosslinking between the WG segments and the amorphous components in WF were facilitated by such severe shear deformation. However, WG would be thermally decomposed at high temperatures, resulting in weakened mechanical properties for the WF/WG samples processed at 150 °C. Developing thermally stable amorphous natural polymer additives and examining the effect of increasing shear deformation would be needed before manufacturing trials on industrial scales.

References

Belton, P. S. (1999). On the elasticity of wheat gluten. *Journal of Cereal Science*, *29*, 103–107.

Bogoeva-Gaceva, G., Avella, M., Malinconico, M., Buzatovska, A., Grozdanov, A., Gentile, G., et al. (2007). Natural fiber eco-composites. *Polymer Composites*, *28*, 98–107.

Eichhorn, S. J., & Young, R. J. (2001). The Young's modulus of a microcrystalline cellulose. *Cellulose*, *8*, 197–207.

Horii, F., Hirai, A., & Kitamaru, R. (1987). CP/MAS Carbon-13 NMR spectra of the crystalline components of native celluloses. *Macromolecules*, *20*, 2117–2120.

John, M. J., & Thomas, S. (2008). Biofibres and biocomposites. *Carbohydrate Polymers*, *71*, 343–364.

Klemm, D., Heublein, B., Fink, H. P., & Bohn, A. (2005). Cellulose: Fascinating biopolymer and sustainable raw material. *Angewandte Chemie International Edition*, *44*, 3358–3393.

Lu, X., Zhang, M. Q., Rong, M. Z., Shi, G., & Yang, G. C. (2003). Self-reinforced melt processable composites of sisal. *Composites Science and Technology*, *63*, 177–186.

Newman, R. H. (1999). Estimation of the lateral dimensions of cellulose crystallites using ^{13}C NMR signal strengths. *Solid State Nuclear Magnetic Resonance*, *15*, 21–29.

Nishino, T., Matsuda, I., & Hirao, K. (2004). All-cellulose composites. *Macromolecules*, *37*, 7683–7687.

Ragauskas, A. J., Williams, C. K., Davison, B. H., Britovsek, G., Cairney, J., & Eckert, C. A. (2006). The path forward for biofuels and biomaterials. *Science*, *311*, 484–489.

Reddy, N., & Yang, Y. (2011). Biocomposites developed using water-plasticized wheat gluten as matrix and jute fibres as reinforcement. *Polymer International*, *60*, 711–716.

Sjostrom, E. (1993). *Wood chemistry fundamentals and applications*. Academic Press. Inc.

Tanaka, F., & Iwata, T. (2006). Estimation of the elastic modulus of cellulose crystal by molecular mechanics simulation. *Cellulose*, *13*, 509–517.

VanderHart, D. L., & Atalla, R. H. (1984). Studies of microstructure in native cellulose using solid-state ^{13}C NMR. *Macromolecules*, *17*, 1465–1472.

Wang, Y., & Zhang, L. (2009). Blends and composites based on cellulose and natural polymers. In L. Yu (Ed.), *Biodegradable polymer blends and composites from renewable resources* (pp. 129–161). Wiley, A John Wiley & Sons Inc (Chapter 6).

Zhang, X., & Solomon, D. H. (1998). The chemistry of novolac resins: Part 5, reactions of benzoxazines intermediates. *Polymer*, *39*, 399–404.

Zhang, X., Do, M. D., Hoobin, P., & Burgar, I. (2006). The phase composition and molecular motions of plasticized wheat gluten-based biodegradable polymer materials studied by solid-state NMR spectroscopy. *Polymer*, *47*, 5888–5896.

Zhang, X., Hoobin, P., Burgar, I., & Do, M. D. (2006b). pH effect on the mechanical performance and phase mobility of thermally processed wheat gluten-based natural polymer materials. *Biomacromolecules*, *7*, 3466–3473.

Zhang, X., Hoobin, P., Burgar, I., & Do, M. D. (2006c). Chemical modification of wheat protein-based natural polymers: Crosslinking effect on mechanical properties and phase structures. *Journal of Agricultural and Food Chemistry*, *54*, 9858–9865.

Zhang, X., Gao, D., Wu, X., & Xia, K. (2008). Bulk plastic materials obtained from processing raw powders of renewable natural polymers via back pressure equal channel angular consolidation (BP-ECAC). *European Polymer Journal*, *44*, 780–792.

Zhang, X., Do, M. D., Casey, P., Sulistio, A., Qiao, G. G., Lundin, L., et al. (2010). Chemical crosslinking gelatin with natural phenolic compounds as studied by high-resolution NMR spectroscopy. *Biomacromolecules*, *11*, 1125–1132.

Zhang, X., Wu, X., Gao, D., & Xia, K. (2012). Bulk cellulose plastic materials from processing cellulose powder using back pressure equal channel angular pressing. *Carbohydrate Polymers*, *87*, 2470–2476.

Zhang, X., Wu, X., & Xia, K. (2013). Cellulose-wheat gluten bulk plastic materials produced from processing raw powder by severe shear deformation. *Carbohydrate Polymers*, *92*, 2206–2211.